Journal of Magnetic Resonance 195 (2008) 196–205

Contents lists available at ScienceDirect

Journal of Magnetic Resonance

journal homepage: www.elsevier.com/locate/jmr

Schonland ambiguity in the electron nuclear double resonance analysis of hyperfine interactions: Principles and practice

H. Vrielinck [a,1], H. De Cooman [a,c,2], M.A. Tarpan [a,2], E. Sagstuen [b], M. Waroquier [c], F. Callens [a,*]

[a] Ghent University, Department of Solid State Sciences, Krijgslaan 281-S1, B-9000 Gent, Belgium
[b] University of Oslo, Department of Physics, P.O. Box 1048 Blindern, N-0316 Oslo, Norway
[c] Ghent University, Center for Molecular Modeling, Proeftuinstraat 85, B-9000 Gent, Belgium

ARTICLE INFO

Article history:
Received 18 June 2008
Revised 12 August 2008
Available online 23 September 2008

Keywords:
ENDOR
Hyperfine couplings
Fitting results
Ambiguity
DFT calculations

ABSTRACT

For the analysis of the angular dependence of electron paramagnetic resonance (EPR) spectra of low-symmetry centres with $S = 1/2$ in three independent planes, it is well-established—but often overlooked—that an ambiguity may arise in the best-fit $\overleftrightarrow{g}$ tensor result. We investigate here whether a corresponding ambiguity also arises when determining the hyperfine coupling (HFC) $\overleftrightarrow{A}$ tensor for nuclei with $I = 1/2$ from angular dependent electron nuclear double resonance (ENDOR) measurements. It is shown via a perturbation treatment that for each set of M_S ENDOR branches two best-fit $\overleftrightarrow{A}$ tensors can be derived, but in general only one unique solution simultaneously fits both. The ambiguity thus only arises when experimental data of only one M_S multiplet are used in analysis or in certain limiting cases. It is important to realise that the ambiguity occurs in the ENDOR frequencies and therefore the other best-fit result for an ENDOR determined $\overleftrightarrow{A}$ tensor depends on various details of the ENDOR experiment: the M_S state of the fitted transitions, the microwave frequency (or static magnetic field) in the ENDOR measurements and the rotation planes in which data have been collected. The results are of particular importance in the identification of radicals based on comparison of theoretical predictions of HFCs with published literature data. A procedure for obtaining the other best-fit result for an ENDOR determined $\overleftrightarrow{A}$ tensor is outlined.

1. Introduction

Determining the principal values and directions of the $\overleftrightarrow{g}$ tensor from the angular dependence of spectra is one of the central problems of single crystal electron paramagnetic resonance (EPR) spectroscopy. Already in 1959, Schonland [1] pointed out an ambiguity arising when determining the $\overleftrightarrow{g}$ tensor in the spin Hamiltonian

$$\widehat{H}_S = \mu_B \vec{B} \cdot \overleftrightarrow{g} \cdot \widehat{\vec{S}} \tag{1}$$

for low-symmetry paramagnetic centres with effective spin $S = 1/2$ in crystals with orthorhombic and monoclinic symmetry (although the problem is not restricted to these classes of crystal symmetry). For such crystals, $\overleftrightarrow{g}$, which we assume to be symmetric [2] and represented in an orthonormal reference frame fixed to the crystal, is commonly determined by analysing the angular dependence of the EPR spectrum in the three crystallographic planes $\{ab\}$, $\{bc\}$ and $\{ca\}$. For monoclinic crystals with $\langle b\rangle$ as twofold rotation axis or $\{ac\}$ as mirror plane, $\langle a\rangle$ and $\langle c\rangle$, and hence also $\{ab\}$ and $\{bc\}$ are not perpendicular to one another. It is sometimes more convenient to perform experiments in the $\{a^*b\}$ and/or $\{bc^*\}$ ($\langle a^*\rangle$ perpendicular to $\langle b\rangle$ and $\langle c\rangle$, $\langle c^*\rangle$ perpendicular to $\langle a\rangle$ and $\langle b\rangle$) planes, instead of in $\{ab\}$ and $\{bc\}$, respectively. Schonland demonstrated that from data analysis in three planes of this kind two distinct best-fit solutions can be found, differing both in principal values and eigenvectors. In this paper we will refer to these two solutions as Schonland conjugate tensors. Only one of them corresponds to the $\overleftrightarrow{g}$ tensor of the paramagnetic defect under study, the other is a fitting result without physical meaning. Outside of these three planes, the EPR positions calculated for the two solutions may differ considerably and a straightforward solution to the problem is to complete the experiments by measurements in a fourth, skewed plane. Recording the powder EPR spectrum can also lift the ambiguity, because the principal g values—but in general not the directions—can be directly determined from it. In addition, Morton and Preston [2] described a procedure to avoid this ambiguity in single crystal EPR by choice of the rotation planes using a two-circle goniometer.

Later papers on $\overleftrightarrow{g}$ tensor analysis and EPR textbooks (see e.g. [3,4]) have extended the work of Schonland and further documented possible ambiguities in fitting results. Nonetheless, in experimental EPR literature, this problem is often not recognised. Yet, it may have serious implications when principal values and directions of the wrong $\overleftrightarrow{g}$ tensor would be interpreted theoretically to infer the molecular structure of the paramagnetic defect.

* Corresponding author. Tel.: +32 9 264 43 52; fax: +32 9 264 49 96.
E-mail address: Freddy.Callens@UGent.be (F. Callens).
[1] Postdoctoral Fellow of the Flemish Research Foundation (FWO-Vlaanderen).
[2] Research Assistant of the Flemish Research Foundation (FWO-Vlaanderen).

1090-7807/$ - see front matter © 2008 Elsevier Inc. All rights reserved.
doi:10.1016/j.jmr.2008.09.017

In a similar way as for $\overleftrightarrow{g}$, one may want to determine the hyperfine coupling (HFC) A tensor—which we also assume to be symmetrical—for a nucleus with $I = 1/2$ in the spin Hamiltonian ($S = 1/2$)

$$\widehat{H}_S = \mu_B \vec{B} \cdot \overleftrightarrow{g} \cdot \widehat{\vec{S}} + \widehat{\vec{S}} \cdot \overleftrightarrow{A} \cdot \widehat{\vec{I}} - g_N \mu_N \vec{B} \cdot \widehat{\vec{I}} \tag{2}$$

from the angular dependence of electron nuclear double resonance (ENDOR) spectra. Hence, one may wonder if for a corresponding set of experimental data an analogous Schonland-type ambiguity in the best-fit solution exists. This problem has, to the best of our knowledge, neither been treated yet from a theoretical nor from a practical viewpoint in the literature, although it has been recognised that in the analysis of EPR spectra, treating the HF interaction as a perturbation to first order, the ambiguity does arise [3–5]. Our interest in this matter, and particularly in the ENDOR analysis, arises from our study of the structure of radiation-induced radicals in single crystals of mono- and disaccharides [6–9] and other bio-organic molecules [10–13]. In such crystals, each radical formed is characterised by a set of proton (^{1}H) HFC tensors, whose principal values and directions are determined from angular dependent ENDOR experiments, and which are assigned to this particular radical based on ENDOR-induced EPR measurements. From a set of semi-empirical rules and equations [14] information on the chemical identity of the radical can be inferred from the size of the principal HFC values, the tensor anisotropy and principal directions. This is, however, often still insufficient for a complete identification of the radical structure. In recent years, "first principles" calculations of $\overleftrightarrow{A}$ tensors based on density functional theory (DFT) have become increasingly fast and reliable. In our research of these systems, the comparison between calculated and experimental principal HFC values and eigenvectors for proposed radical structures has become a crucial step in the radical model assignment.

Both semi-empirical theoretical interpretation and identification based on comparison with computational results rely strongly on an accurate determination of experimental tensors. From this viewpoint it is important to know whether or not a Schonland-type ambiguity exists, because only the physically relevant tensor provides information on the radical model and can be reproduced in calculations, not its Schonland conjugate. In this paper, we explore this question.

Throughout this paper, we choose $(\vec{e}_a, \vec{e}_b, \vec{e}_c)$ as the reference frame for representation of tensors for orthorhombic crystals and $(\vec{e}_a, \vec{e}_b, \vec{e}_{c^*})$ for monoclinic crystals. Where this choice makes a difference, the results in a $(\vec{e}_{a^*}, \vec{e}_b, \vec{e}_c)$ reference frame are also mentioned. The simulations shown in Section 3 are obtained by diagonalisation of the spin Hamiltonians (1) and (2) using the EasySpin routines [15] in Matlab. These simulations demonstrate that for HFC tensors of practical interest in the study of radiation defects in bio-organic molecules like saccharides, the use of first order perturbation theory in the formulae derived for calculating Schonland conjugate tensors is sufficiently accurate.

2. Principle of Schonland ambiguity for the HFC tensor: perturbation theory approach

Schonland [1] demonstrated that in any rotation plane the angular dependence of the EPR resonance field $B_0 = h\nu_{MW}/g\mu_B$ ($\vec{B} = B_0\vec{l}$), on the rotation angle θ follows

$$g^2 = \vec{l} \cdot \overleftrightarrow{g} \cdot \overleftrightarrow{g} \cdot \vec{l}^{\mathrm{T}} = \alpha + \beta \cos 2\theta + \gamma \sin 2\theta \tag{3}$$

α, β and γ (being expressed also by the elements of the squared $\overleftrightarrow{g}$ tensor) can directly be calculated from the maximum and minimum g value encountered in this plane, and the angle θ at which the maximum g value occurs [1,3]. Ignoring for the moment the possible presence of symmetry-related centres (site splitting), whose $\overleftrightarrow{g}$ tensors are related to those of the "original" centre by the symmetry operations of the crystal's point group [4], the occurrence of two best-fit solutions springs from an ambiguity in the positive rotation sense in the planes, thus in the sign of θ or, alternatively, in the sign of γ. Indeed from Eq. (3) it follows that $g^2(\alpha,\beta,\gamma,-\theta) = g^2(\alpha,\beta,-\gamma,\theta)$. Rotation senses may, however, not be clear from EPR experiments alone. When analysing data in three rotation planes, in two of them the sign of γ may be chosen without important consequences, but this fixes the choice in the third plane. When the measurements are performed on three different crystals, it is however not a priori clear which sign has to be chosen. A further complication occurs if, due to site splitting in at least two of the planes, two branches occur in the angular dependence. Then it cannot be decided which branches should be fit together (see further in Section 3.1 and Fig. 1). The two best-fit solutions thus follow from the two sign choices for γ in the third rotation plane.

From these considerations, it is clear that an ambiguity may arise for the $\overleftrightarrow{A}$ tensor if the ENDOR resonance frequencies in an arbitrary plane show an angular dependence similar to Eq. (3). Under the assumption that the HF splitting is small with respect to the resonance field (high-field approximation), the eigenvalues of the spin Hamiltonian (2) are calculated as (see e.g. [16–18])

$$\begin{aligned} E(M_S, M_I) &= \mu_B g B_0 M_S + K(M_S) M_I \\ K^2(M_S) &= \vec{l} \cdot \overleftrightarrow{K}(M_S) \cdot \left[\overleftrightarrow{K}(M_S)\right]^{\mathrm{T}} \cdot \vec{l}^{\mathrm{T}} \\ \overleftrightarrow{K}(M_S) &= \frac{\overleftrightarrow{g} \cdot \overleftrightarrow{A}}{g} M_S - g_N \mu_N B_0 \overleftrightarrow{1}_{3\times 3} \end{aligned} \tag{4}$$

and two ENDOR transitions occur at $|K(\pm 1/2)|$. Formally, $\overleftrightarrow{K} \cdot \overleftrightarrow{K}^{\mathrm{T}}$ takes over the role of $\overleftrightarrow{g} \cdot \overleftrightarrow{g}$ in the left hand side of Eq. (3), but in general the angular dependence is more complicated, as also g exhibits angular dependence. However, in the data analysis for radicals in organic solids, the (often not analysed) $\overleftrightarrow{g}$ tensor is nearly isotropic and all ENDOR measurements are performed at approximately the same resonance field B_0, so that

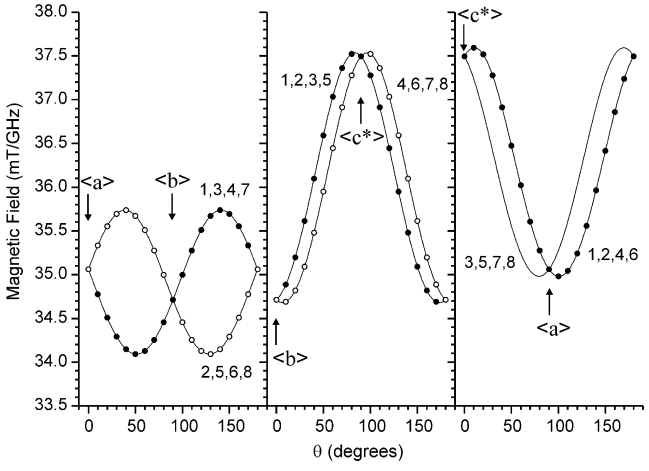

Fig. 1. Angular dependence of EPR field positions normalised to 1 GHz microwave frequency (in units mT/GHz) in three perpendicular rotation planes {ab}, {bc^*} and {c^*a}. *Symbols:* Calculated for a non-symmetric paramagnetic centre with $S = 1/2$ in a crystal with monoclinic symmetry, exhibiting the $\overleftrightarrow{g}$ tensor 1 in Table 1 for one of the symmetry-related centres (filled circles) and tensor 6 for the other (open circles). Note that in the {c^*a} plane the resonance fields for the two symmetry-related centres coincide. *Full lines:* Calculated for $\overleftrightarrow{g}$ tensors 1–8 in Table 1, labels refer to the tensor number in Table 1. The simulations illustrate that changing the sign of the M_{ij} element corresponds to changing the rotation sense in the ij plane ($i,j = 1,2,3$, see text).

$$\overleftrightarrow{K}(M_S) = \left[\overleftrightarrow{K}(M_S)\right]^{\mathrm{T}} = M_S \overleftrightarrow{A} - g_N \mu_N B_0 \overleftrightarrow{1}_{3\times 3} \tag{5}$$

is a very good approximation. The angular dependence of the resonance frequencies within each M_S multiplet, $|K(\pm 1/2)|$, then follows (3)

$$K^2(M_S) = \vec{l} \cdot \overleftrightarrow{K}(M_S) \cdot \overleftrightarrow{K}(M_S) \cdot \vec{l}^{\mathrm{T}} = \alpha + \beta \cos 2\theta + \gamma \sin 2\theta \tag{6}$$

Hence, as for the $\overleftrightarrow{g}$ tensor, for each $\overleftrightarrow{K}(M_S)$ tensor, two best-fit solutions can be derived from angular dependences in three planes. Via Eq. (5) an ambiguity in $\overleftrightarrow{K}(M_S)$ immediately leads to an ambiguity in $\overleftrightarrow{A}$ as well. However, in order to fit the resonance frequencies in both M_S multiplets, the $\overleftrightarrow{A}$ tensors calculated from the best-fit $\overleftrightarrow{K}(1/2)$ and $\overleftrightarrow{K}(-1/2)$ solutions should coincide, and we will illustrate in Section 3 that in general this is only the case for one of the solutions. Hence, in principle a Schonland ambiguity does not occur when determining hyperfine interactions from the angular dependence of ENDOR spectra. In practice, however, very often the nuclear resonances in only one of the multiplets can be used for analysis, and the problem of finding two best-fit $\overleftrightarrow{A}$ solutions to the data reappears.

In addition, there are limiting cases where the Schonland conjugate $\overleftrightarrow{A}$ tensors calculated for the two M_S multiplets are nearly identical. When the HF interaction is small compared to twice the nuclear Zeeman energy at all orientations (requiring a small isotropic value and a sufficiently small anisotropy), by neglecting terms quadratic in the HFC tensor Eq. (4) yields that the ENDOR frequencies are found at

$$\begin{aligned} &|K(M_S)| \approx |AM_S - g_N \mu_N B_0| \\ &A = \vec{l} \cdot \overleftrightarrow{A} \cdot \vec{l}^{\mathrm{T}} \end{aligned} \tag{7}$$

and $\overleftrightarrow{A}$ takes over the role of $\overleftrightarrow{K} \cdot \overleftrightarrow{K}$ in Eq. (6). This limiting case often occurs in practice, e.g. for γ-protons, especially when experiments are carried out at microwave frequencies higher than X-band (10 GHz).

In the opposite case of large HFCs, neglect of the term quadratic in the nuclear Zeeman energy in (4) leads to

$$|K(M_S)| = \left| \sqrt{\vec{l} \cdot \overleftrightarrow{A} \cdot \overleftrightarrow{A} \cdot \vec{l}^{\mathrm{T}}} M_S - g_N \mu_N B_0 \frac{\vec{l} \cdot \overleftrightarrow{A} \cdot \vec{l}^{\mathrm{T}}}{\sqrt{\vec{l} \cdot \overleftrightarrow{A} \cdot \overleftrightarrow{A} \cdot \vec{l}^{\mathrm{T}}}} \right| \tag{8}$$

If the anisotropy in $\overleftrightarrow{A}$ is small, it may be verified that for all magnetic field orientations $\vec{l} \cdot \overleftrightarrow{A} \cdot \vec{l}^{\mathrm{T}} \approx \sqrt{\vec{l} \cdot \overleftrightarrow{A} \cdot \overleftrightarrow{A} \cdot \vec{l}^{\mathrm{T}}}$, and a Schonland ambiguity arises in $\overleftrightarrow{A} \cdot \overleftrightarrow{A}$. Such HF tensors are typically observed for β-protons and the requirements for neglecting the high-order terms in the nuclear Zeeman frequency are best fulfilled at relatively low microwave frequencies. An ambiguity in $\overleftrightarrow{A} \cdot \overleftrightarrow{A}$ is also encountered when analysing the angular dependence of the HF splitting in the EPR spectrum for large A, when the nuclear Zeeman interaction is completely neglected [4,5].

It is worth noting that in these two limiting cases Schonland conjugation becomes independent of B_0 or the microwave frequency (see also Section 3.1.3). In view of certain analogies in the calculation procedures for the Schonland conjugate of a $\overleftrightarrow{g}$ tensor (see Section 3.1.1), one might be tempted to believe that the Schonland conjugate of an $\overleftrightarrow{A}$ tensor can in general be found in this way. This is, however, contradicted by Eqs. (5) and (6). In Section 3.1.2 we illustrate the consequences of making use of the formulae valid in limiting cases for a system where HF and nuclear Zeeman interactions have the same order of magnitude.

The assumptions under which Eq. (5) is derived appear to restrict its scope, although in practice for a lot of systems it may safely be applied. It has been stated that for moderate $\overleftrightarrow{g}$ anisotropy (total anisotropy of the order of 10% of the average g value), as encountered for many free radicals and simple transition metal complexes, neglecting it introduces errors in obtained $\overleftrightarrow{A}$ tensors in the order of experimental accuracy [4]. The simulations shown in the next section, based on full diagonalisation of the spin Hamiltonian (2), justify *a posteriori* that the order of perturbation used here is appropriate for HFCs up to ~100 MHz at moderate (~10 GHz, X-band) and higher microwave frequencies. This is in part a result of the fact that the higher order corrections to the ENDOR frequencies for Schonland conjugate tensors are very similar.

3. Practice: finding Schonland conjugate forms and selecting the right solution

In this section, we illustrate the consequences of Schonland ambiguity for the $\overleftrightarrow{A}$ tensor in the analysis of angular dependent ENDOR spectra for various choices of the three rotation planes. Throughout this section experimental alternatives to performing measurements in a fourth independent plane are offered to select the correct form for the $\overleftrightarrow{A}$ tensor out of the two Schonland conjugate possibilities. The first subsection also comprises a recapitulation of the (simpler, but more essential) problem for the $\overleftrightarrow{g}$ tensor for readers less familiar with the problem discussed by Schonland [1].

Another important purpose of this section is to discuss how the other best-fit tensor to the ENDOR data can be found for literature cases where one suspects the wrong Schonland conjugate $\overleftrightarrow{A}$ tensor was chosen. It is clear that the ENDOR spectroscopist, having the experimental data and simulation and fitting tools at hand, can find the other tensor by fitting, changing the rotation sense in one of the planes in which spectra have been recorded. We present here an analytical and fast way of calculating the Schonland conjugate tensor, based on the first order perturbation expressions in Eq. (4). It is important to bear in mind that for an ENDOR experiment, the origin of the ambiguity is in the ENDOR frequencies and hence is directly described by the $\overleftrightarrow{K}$ tensor (Eqs. (5) and (6)) and only indirectly by the $\overleftrightarrow{A}$ tensor. On the other hand, it is the $\overleftrightarrow{A}$ tensor that bears information on the radical structure and that we are ultimately interested in, not $\overleftrightarrow{K}$.

As will be shown, the calculations imply a sign-indetermination in the principal values of $\overleftrightarrow{K}$, which introduces further ambiguity in the analysis. As this type of ambiguity also appears when determining other electron magnetic resonance properties (e.g. $\overleftrightarrow{g}$ and/or $\overleftrightarrow{A}$ from EPR spectra), we choose to follow a practical approach, which works quite well for the examples given. Moreover, it has recently been shown that pulsed ENDOR at high field [19] and/or for special pulse sequences [20,21] allows determining absolute signs of HFCs. Relative signs of different couplings, on the other hand, may be obtained from electron nuclear nuclear triple resonance experiments [4].

We will restrict ourselves to three cases often encountered in practice. The first is that of data points collected in three orthogonal planes, more specifically the $\{ab\}$, $\{bc\}$ and $\{ca\}$ planes for orthorhombic and $\{ab\}$, $\{bc^*\}$ and $\{c^*a\}$ planes for monoclinic crystals. In the second subsection, extension to two cases relevant for monoclinic crystals are discussed: analysis of data in the $\{ab\}$, $\{bc\}$ and $\{c^*a\}$ planes, and in the $\{a^*b\}$, $\{bc^*\}$ and $\{c^*a\}$ planes. For all these cases, due to the occurrence of site splitting, the ambiguity cannot be lifted by explicit knowledge of the rotation sense in the planes. Finally, in Section 3.3, we show that when lifting the degeneracy of the transitions, the Schonland ambiguity in principle is also lifted.

Throughout this section, we denote the tensor in which a Schonland-type ambiguity may arise ($\overleftrightarrow{g} \cdot \overleftrightarrow{g}, \overleftrightarrow{K}(M_S) \cdot \overleftrightarrow{K}(M_S)$, and in limiting cases $\overleftrightarrow{A}$ or $\overleftrightarrow{A} \cdot \overleftrightarrow{A}$) as $\overleftrightarrow{M}$ and its elements as M_{ij} ($i,j = 1,2,3$, with 1 corresponding to $\langle a \rangle$, 2 to $\langle b \rangle$ and 3 to $\langle c^{(*)} \rangle$). The elements of a Schonland conjugate tensor will be called $\tilde{M}_{ij}$ and those of a tensor related to M by crystallographic point-group symmetry operations $\overline{M}_{ij}$.

3.1. Analysis of data in three orthogonal planes: {ab}, {bc$^{(*)}$}, {c$^{(*)}$a}

As explained by Schonland [1] and in Section 2, the occurrence of two best-fit solutions is the result of an ambiguity in the sign of the γ parameters of Eqs. (3) or (6), related to the sense of rotation in the three planes. Labelling the α, β and γ parameters with 3 for rotation in the {ab} plane, with 1 for {$bc^{(*)}$} and with 2 for {$c^{(*)}a$}, one finds (see Ref. [1])

$$\begin{aligned} M_{11} &= \alpha_3 + \beta_3 \quad M_{22} = \alpha_3 - \beta_3 \quad M_{12} = \gamma_3 \\ M_{22} &= \alpha_1 + \beta_1 \quad M_{33} = \alpha_1 - \beta_1 \quad M_{23} = \gamma_1 \\ M_{33} &= \alpha_2 + \beta_2 \quad M_{11} = \alpha_2 - \beta_2 \quad M_{13} = \gamma_2 \end{aligned} \tag{9}$$

For this particular choice of planes, i.e. the principal planes of the reference frame in which the $\overleftrightarrow{g}$ and/or $\overleftrightarrow{A}$ tensors are represented, the ambiguity thus lies in the sign of the off-diagonal elements of the $\overleftrightarrow{M}$ tensor.

3.1.1. Illustration for the g tensor

We briefly illustrate the problem for the $\overleftrightarrow{g}$ tensor. In Table 1, the principal g values and directions for the eight possible sign combinations of the off-diagonal elements of $\overleftrightarrow{M} = \overleftrightarrow{g} \cdot \overleftrightarrow{g}$ are given. $\overleftrightarrow{g}$ is calculated from $\overleftrightarrow{M}$ as its positive symmetrical square root, i.e. the tensor with the same principal directions and whose principal values are the positive square roots of those of $\overleftrightarrow{M}$. It is well known that the sign of the principal g values cannot be determined in regular EPR experiments making use of linearly polarised microwaves, so in principle both positive and negative square roots should be considered. However, negative g values are not so common and practically excluded in the context of radicals in organic crystals, where only small deviations from $g = 2$ are expected. Hence, in this example it makes sense to restrict the choice of signs to positive. In Table 1 one can verify that the eight tensors split up in two sets (1,5,6,7 and 2,3,4,8). Within a set the tensors are transformed into one another by changing the signs of an even number of off-diagonal elements. These transformations are equivalent to the symmetry operations of the orthorhombic group (unity operator and twofold rotations around the x, y and z axes). As a consequence, all four tensors within a set have the same principal values. Changing the sign of an odd number of off-diagonal elements in $\overleftrightarrow{M}$ transforms a $\overleftrightarrow{g}$ tensor of one set into one of the other. No symmetry operation can be found which transforms two tensors belonging to different sets into one another, which is immediately clear, because they have different principal values. The fact that changing an odd number of off-diagonal elements in sign leads to a tensor with different principal values can be readily understood considering that the secular equation for finding the principal values of $\overleftrightarrow{M} = \overleftrightarrow{g} \cdot \overleftrightarrow{g}$ contains only one term (part of the constant term) sensitive to the signs of the off-diagonal elements, more specifically $M_{12}M_{13}M_{23}$. This further implies that possible ambiguity with respect to the principal values disappears, if at least one of these off-diagonal elements is zero (which happens e.g. if the radical has higher symmetry).

Table 1
Principal values and directions of the positive symmetrical square roots of the $\overleftrightarrow{g} \cdot \overleftrightarrow{g}$ tensors obtained by considering the eight possible sign combinations of the off-diagonal elements for $\overleftrightarrow{g} \cdot \overleftrightarrow{g}$ calculated from the tensor in row 1

		Principal value	Direction cosines with respect to		
			a	b	c^*
1	Original M	1.9000	0.1632	0.0594	0.9848
		2.0000	0.7589	−0.6454	−0.0868
		2.1000	0.6304	0.7615	−0.1504
2	$\tilde{M}_{12} = -M_{12}$	1.8957	0.2338	0.1740	0.9566
		2.0086	0.7399	0.6064	−0.2912
		2.0957	−0.6307	0.7759	0.0130
3	$\tilde{M}_{13} = -M_{13}$	1.8957	−0.2338	0.1740	0.9566
		2.0086	−0.7399	0.6064	−0.2912
		2.0957	−0.6307	−0.7759	−0.0130
4	$\tilde{M}_{23} = -M_{23}$	1.8957	0.2338	−0.1740	0.9566
		2.0086	−0.7399	0.6064	0.2912
		2.0957	−0.6307	−0.7759	0.0130
5	$\tilde{M}_{12} = -M_{12}$	1.9000	−0.1632	0.0594	0.9848
	$\tilde{M}_{13} = -M_{13}$	2.0000	−0.7589	−0.6454	−0.0868
		2.1000	0.6304	−0.7615	0.1504
6	$\tilde{M}_{12} = -M_{12}$	1.9000	0.1632	−0.0594	0.9848
	$\tilde{M}_{23} = -M_{23}$	2.0000	−0.7589	−0.6454	0.0868
		2.1000	0.6304	−0.7615	−0.1504
7	$\tilde{M}_{13} = -M_{13}$	1.9000	−0.1632	−0.0594	0.9848
	$\tilde{M}_{23} = -M_{23}$	2.0000	0.7589	−0.6454	0.0868
		2.1000	0.6304	0.7615	0.1504
8	$\tilde{M}_{12} = -M_{12}$	1.8957	−0.2338	−0.1740	0.9566
	$\tilde{M}_{13} = -M_{13}$	2.0086	0.7399	0.6064	0.2912
	$\tilde{M}_{23} = -M_{23}$	2.0957	−0.6307	0.7759	−0.0130

Tensors 1, 5, 6 and 7, form a set with identical principal values, obtained by changing the sign of an even number of off-diagonal elements. The second set, containing 2, 3, 4 and 8, is obtained by changing the sign of an odd number of off-diagonal elements. The tensors within each set are transformed into one another by a symmetry operation of the orthorhombic group: sign changes in the elements M_{ij} and M_{jk} are equivalent to a twofold rotation around the $\langle j \rangle$ axis or a mirror operation through the {ik} plane ($i,j,k = a,b,c^*$).

In Fig. 1 the calculated angular dependence for these eight tensors (solid lines) is compared to that expected to be measured for a non-symmetric paramagnetic centre (i.e. with triclinic or C_1 symmetry) in a monoclinic crystal with the first tensor in Table 1 as $\overleftrightarrow{g}$, for the first (filled circles) and the sixth tensor for the symmetry related centre (open circles). Fig. 1 clearly illustrates:

(i) The degeneracy of the resonance fields in the {c^*a} plane.
(ii) Changing the sign of the off-diagonal element M_{ij} is equivalent to changing the rotation sense in the {ij} plane.
(iii) Two symmetry operations of the orthorhombic group do not belong to the monoclinic group. The resonance fields calculated for $\overleftrightarrow{g}$ tensors 3, 5, 7 and 8 do not match the angular dependence in the {c^*a} plane. In the following we continue with the example of a non-symmetric centre in a monoclinic crystal and will therefore only consider sign changes in the M_{12} or M_{23} elements.
(iv) The two Schonland conjugate solutions (two sets of two tensors, (1,6) and (2,4), related within a set by monoclinic symmetry operations) fit the "experimental" points equally well and it is thus not possible to decide from these data which $\overleftrightarrow{g}$ tensor is the correct form and which only fits in these three planes.

Fig. 1 also illustrates that in this example, where site splitting occurs, the ambiguity is essential: even if the rotation sense in the three planes is known, it cannot be decided from experiment whether the angular dependence of the filled circles in the {ab} plane should be combined with that of the filled circles in the {bc^*} plane, leading to tensor 1, or with that of the open circles, leading to the Schonland conjugate tensor 4.

3.1.2. Schonland conjugate of a HFC tensor

We now move on to the ambiguity for the $\overleftrightarrow{A}$ tensor and focus on the analysis of ^{1}H couplings by ENDOR spectroscopy. We assume that an ambiguity in the fitting result may arise because the transitions within only one of the M_S multiplets were fitted. Most often, these are the transitions occurring at the higher frequencies. For tensors with positive principal values, and hence a positive trace ($\mathrm{Tr}(A) = 3A_{\mathrm{iso}}$), as for β-protons, these are the $M_S = -1/2$ transitions, for α-protons with negative principal values and A_{iso}, they are those in the $M_S = 1/2$ multiplet. As $g_N(^1\mathrm{H}) > 0$, in either case

$$\overleftrightarrow{K}_{\text{high}} = -\text{sign}(A_{\text{iso}})\frac{\overleftrightarrow{A}}{2} - g_N\mu_N B_0 \overleftrightarrow{1}_{3\times 3} \tag{10}$$

Like for $\vec{g}$, Schonland conjugate forms of $\overleftrightarrow{K}_{\text{high}}$, designated $\widetilde{\overleftrightarrow{K}}_{\text{high}}$, can now be found by changing either the 12 or the 23 element of $\overleftrightarrow{M} = \overleftrightarrow{K}_{\text{high}} \cdot \overleftrightarrow{K}_{\text{high}}$ and taking its symmetrical square root. However, an important complication arises immediately, because the square root operation can only be performed when all three principal values of $\widetilde{\overleftrightarrow{K}} \cdot \widetilde{\overleftrightarrow{K}}$ are positive, which is most often the case, but not in general. Negative principal values of $\widetilde{\overleftrightarrow{K}} \cdot \widetilde{\overleftrightarrow{K}}$, however, indicate that a Schonland conjugate tensor $\widetilde{\overleftrightarrow{A}}$ cannot be found in such cases, as it would have complex principal values. In addition, for each principal $\widetilde{\overleftrightarrow{K}}$ value both the positive and the negative square root should in principle be considered. The problem of determining the signs of the principal values already occurs for $\overleftrightarrow{K}$ in a first order analysis of ENDOR data within only one of the M_S multiplets, but inspection of the simulations for all possible sign combinations usually allows the selection of one solution as most plausible. This gives rise to one $\overleftrightarrow{A}$ tensor solution, completely determined except for a possible overall sign reversal. When for some orientations the ENDOR frequencies of the other multiplet are also observed, the ambiguity in the relative signs of the $\overleftrightarrow{A}$ tensor usually vanishes completely.

Returning to the problem of finding the Schonland conjugate form of $\overleftrightarrow{K}_{\text{high}}$, except when at least one of the principal HFC values has a sign opposite to that of A_{iso} and its magnitude is larger than or comparable to $2g_N\mu_N B$, all principal values of $\overleftrightarrow{K}_{\text{high}}$ are negative and it is safe to assume that those of $\widetilde{\overleftrightarrow{K}}_{\text{high}}$ are all negative as well. From the thus obtained tensor the Schonland conjugate tensor $\widetilde{\overleftrightarrow{A}}$ can be calculated by reversing Eq. (10)

$$\widetilde{\overleftrightarrow{A}} = -2\left(\widetilde{\overleftrightarrow{K}}_{\text{high}} + g_N\mu_N B_0 \overleftrightarrow{1}_{3\times 3}\right)\text{sign}(A_{\text{iso}}) \tag{11}$$

In the second row of Table 2 we show the principal values and directions of the resulting tensor Schonland conjugate to that given in the first row, for $g_N\mu_N B_0 = 14.9$ MHz ($B_0 = 350$ mT or $g = 2$ at 9.80 GHz, X-band), by changing the sign of M_{12}, i.e. considering ambiguity in the sign of γ_3. As an illustration, the procedure for obtaining the original tensor in row 1 of Table 2 from the Schonland conjugate form in row 2 is schematically represented in the Appendix. The original tensor is chosen to have considerable anisotropy and such principal values that for low to moderate microwave frequencies (e.g. X- or Q-band: 34 GHz) the HF and nuclear Zeeman interaction terms have the same order of magnitude. Moreover, the shape of tensor 1 is typical of an α-proton (provided that the signs of all principal values are negative). It is noticeable that the Schonland conjugate tensor 2 may well be interpreted as arising from a β-hydroxyl proton [12,13,22]. This illustrates that Schonland ambiguity can indeed have serious consequences for the radical model selection.

In the third row of Table 2 the Schonland conjugate tensor calculated from the low frequency ENDOR transitions is shown. It is obtained by considering a sign ambiguity in the 12 element of $\overleftrightarrow{K}_{\text{low}} \cdot \overleftrightarrow{K}_{\text{low}}$, where $\overleftrightarrow{K}_{\text{low}}$ is calculated by reversing the sign of the first term on the right hand side of Eq. (10). The problem of determining the signs of the principal $\widetilde{\overleftrightarrow{K}}$ values is somewhat more difficult here, as $\overleftrightarrow{K}_{\text{low}}$ has positive as well as negative principal values. In principle, all sign combinations should be tested. We have chosen here to present only the result of which the determinant is closest to that of the original tensor, because this property directly appears in the formulae for the second order corrections to the ENDOR resonance frequencies (see e.g. [4]). We recognise, though, that next to the Schonland ambiguity, sign ambiguities may also be very pertinent, especially if $\overleftrightarrow{K}_{\text{low/high}}$ has principal values close to zero. Finally, rows 4 and 5 show the Schonland conjugate forms in the limiting cases with $\overleftrightarrow{M} = \overleftrightarrow{A}$ and $\overleftrightarrow{M} = \overleftrightarrow{A} \cdot \overleftrightarrow{A}$ (see Section 2). In Fig. 2 the calculated ENDOR angular dependences for all these tensors (lines) are compared to those expected to be measured (symbols) for the two symmetry-related centres of a non-symmetric centre in a monoclinic crystal, one of which has a HF interaction characterised by tensor 1 in Table 2.

From Table 2 we conclude that the various conjugate tensors differ strongly both in principal values and directions, not only from the original tensor but also considerably among each other. This presents a serious problem if one wants to validate structural models based on comparison with results from "first principles"

Table 2
Starting with an ENDOR determined HFC tensor $\overleftrightarrow{A}$ in row 1, Schonland conjugate tensors are obtained by considering the ambiguity in the sign of the off-diagonal element M_{12} where the M tensors are constructed according to the different possibilities outlined in Sections 2 and 3.1.2 (Eqs. (5), (7) and (8))

		Principal A values (MHz)	Direction cosines with respect to			
			$\langle a \rangle$	$\langle b \rangle$	$\langle c^* \rangle$	
1	Original $\overleftrightarrow{A}$ tensor	*22.50*	−0.6861	−0.5967	0.4162	
		41.25	−0.6287	0.7742	0.0734	
		60.00	−0.3660	−0.2113	−0.9063	
	$\overleftrightarrow{M}$	Principal $\widetilde{A}$ values (MHz)	Direction cosines with respect to			$\Delta\theta$ (°)
			$\langle a \rangle$	$\langle b \rangle$	$\langle c^* \rangle$	
2	$\overleftrightarrow{K}_{\text{high}} \cdot \overleftrightarrow{K}_{\text{high}}$	*29.58*	−0.8887	0.3478	0.2988	*58.22*
		33.16	0.2014	0.8815	−0.4271	*58.37*
		61.62	−0.4119	−0.3194	−0.8534	*7.39*
3	$\overleftrightarrow{K}_{\text{low}} \cdot \overleftrightarrow{K}_{\text{low}}$	*27.44*	−0.6621	−0.6397	0.3905	*3.19*
		43.48	−0.6587	0.7452	0.1039	*2.96*
		59.86	−0.3574	−0.1884	−0.9147	*1.48*
4	$\overleftrightarrow{A}$	*28.27*	−0.8516	0.4665	0.2391	*66.08*
		32.73	0.3061	0.8128	−0.4956	*66.39*
		62.75	−0.4256	−0.3488	−0.8350	*9.52*
5	$\overleftrightarrow{A} \cdot \overleftrightarrow{A}$	*30.66*	−0.9147	0.1669	0.3680	*47.06*
		33.67	0.0344	0.9396	−0.3406	*47.10*
		61.11	−0.4027	−0.2989	−0.8652	*5.93*

The calculation scheme for obtaining tensor 1 from 2, along with intermediate results, is found in Appendix A. All results are obtained assuming that the resonance frequency data are analysed in the $\{ab\}$, $\{bc^*\}$ and $\{c^*a\}$ rotation planes. Calculations are performed for $g_N\mu_N B_0 = 14.902$ MHz, i.e. $B_0 = 350$ mT, or $g = 2$ at $\nu_{\text{MW}} = 9.8$ GHz. The last column gives the deviation in principal directions with the original tensor in the first row.

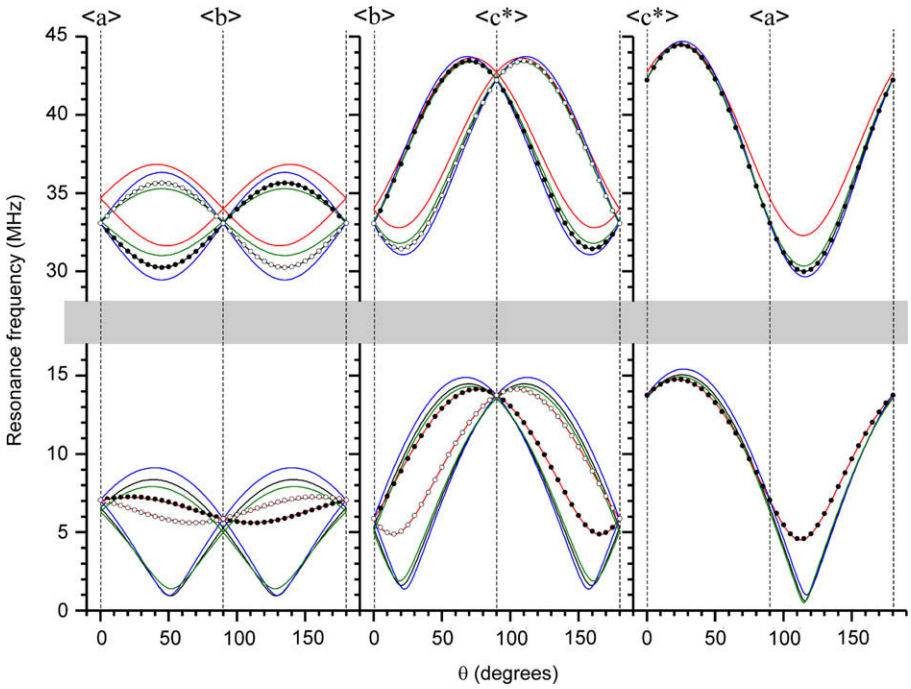

Fig. 2. Angular dependence of ENDOR frequency positions in {*ab*}, {*bc**} and {c^*a} planes, calculated at a microwave frequency of 9.8 GHz (B_0 = 350 mT for g = 2), for a non-symmetric centre with S = 1/2 and isotropic $\vec{\vec{g}}$, interacting with a ^{1}H nucleus in a crystal with monoclinic symmetry. The principal values and directions of the HFC tensors used in the simulations are given in Table 2. *Symbols:* For a nucleus whose interaction is parameterized by the tensor in the first row of Table 2 for one of the sites (filled circles) and by its monoclinic symmetry-related tensor for the other (open circles). *Full lines:* For the two symmetry-related sites of an interaction characterised by the tensor in the second (black), third (red), fourth (blue), and fifth (green) tensor in Table 2.

DFT calculations. Not only should one realise that another best-fit tensor may exist, but one should also carefully consider how to calculate it, based on the details of the performed experiments. Fig. 2 clearly demonstrates that, in this general case with nuclear Zeeman and strongly anisotropic HF interactions of the same order of magnitude, an ambiguity can only arise if one considers only one of the M_S multiplets in the fitting. Furthermore, the conjugate tensors calculated with tensors 4 and 5, this is in the small and large HFC limits, respectively, do not render satisfactory agreement with the data points calculated for the original tensor. These observations are in agreement with our theoretical analysis in Section 2 and demonstrate that a Schonland ambiguity for HFC tensors in principle does not exist. Still, in cases of measurements of the transitions within only one of the M_S states in the three planes here considered, it is impossible to decide between two best-fit solutions (1 and 2 or 1 and 3 in Table 2). Thus, if for an $\vec{\vec{A}}$ tensor given in literature one wants to calculate a Schonland conjugate alternative, in addition to the principal values and directions of the tensor itself, one also needs to know at least if the high or low frequency branches have been considered for analysis. In the following subsections, it will become clear that other details of the experiment are also important for calculating Schonland conjugate tensors.

Analysis procedures to directly obtain the *ij* components of $\vec{\vec{A}}$ by fitting the angular dependence of the difference of the squares of the ENDOR frequencies in the two M_S multiplets ($|K^2(-1/2) - K^2(1/2)| = |g_N\mu_N B_0 \vec{l}\cdot\vec{\vec{A}}\cdot\vec{l}|$, see [4]) may give the impression that an ambiguity with $\vec{\vec{M}} = \vec{\vec{A}}$ may still exist when both ENDOR transitions are considered in the analysis. Fig. 2 (blue lines) shows that in general this ambiguity is lifted by simulation of the actual transition frequencies.

3.1.3. Frequency dependence

Eqs. (10) and (11) demonstrate that, apart from the multiplet fitted, the Schonland conjugate $\vec{\vec{A}}$ tensor also depends on B_0, and thus on the microwave frequency at which experiments were performed. To illustrate this, Fig. 3 shows a comparison between calculated ENDOR frequencies for tensors 1 (open and filled circles) and 2 (fully drawn lines) in Table 2 at 34 GHz, focussing on the high frequency branches (M_S = −1/2). The two patterns do not perfectly match. This indicates that for sufficiently large and anisotropic HF interactions, complementing the measurements in the

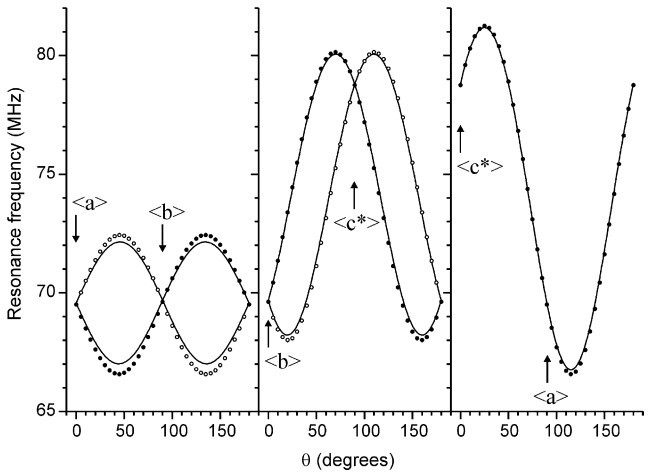

Fig. 3. Angular dependence in {*ab*}, {*bc**} and {c^*a} planes of the high frequency ENDOR branches (M_S = −1/2) for a non-symmetric centre with S = 1/2 interacting with a ^{1}H nucleus in a monoclinic crystal, calculated at a microwave frequency of 34 GHz (1214.6 mT for g = 2). *Symbols:* For one of the symmetry-related sites, the interaction is parameterized by the tensor 1 in Table 2 (filled circles) and for the other by its monoclinic symmetry-related tensor (open circles). *Full lines:* Simulations for the two symmetry-related centres, the interaction of one of which is parameterized by tensor 2 in Table 2. The discrepancy with the angular dependence represented by symbols demonstrates the importance of the microwave frequency in the calculation of the Schonland conjugate form of an $\vec{\vec{A}}$ tensor.

three planes with experiments at another microwave frequency may be considered as an alternative to measuring in a fourth plane for selecting the right best-fit solution, provided that the crystal can be accurately aligned. In general, it appears to be a less discriminating method.

Table 3 illustrates that in the limiting case of relatively small HFCs, i.e. at high microwave frequency, a real Schonland ambiguity arises. The Schonland conjugate $\widetilde{\vec{A}}$ tensors of tensor 1 in Table 2 are calculated from the low and high frequency multiplets at several microwave frequencies. At very high frequency the Schonland conjugate tensors for the high and low frequency branches practically coincide and are nearly equal to tensor 4 in Table 2. At low frequency, we see that in spite of the strong anisotropy, the tensors are also quite similar and, as expected, close to tensor 5 in Table 2. At intermediate frequencies the differences, both in principal values and directions ($\Delta\theta$) are quite considerable. Although not all individual parameters show monotonous relations on the microwave frequency, overall the deviation between the two different Schonland conjugate forms seems to go through a maximum where the HF and nuclear Zeeman interactions are closest in magnitude. These findings are indeed expected from Eqs. (10) and (11) and their analogues for $\widetilde{\vec{K}}_{\text{low}}$.

3.2. Experimental data in non-orthogonal planes for monoclinic crystals

In experiments on monoclinic crystals, it may be more convenient to record angular dependences in the crystallographic {*ab*}, {*bc*} and {*ca*} planes, or to rotate the crystals around their ⟨*a*⟩ ({*bc**} plane), ⟨*b*⟩ ({*c***a*} plane) and ⟨*c*⟩ axes ({*a***b*} plane). Because rotation in a fourth off-axis (tilted) plane allows deciding between Schonland conjugate tensors, changing the rotation planes should also have an influence on the relation between the best-fit tensors.

We assume that the angle between the positive ⟨*c*⟩ and ⟨*a*⟩ axes is $\beta = 90° + \delta$. Hence, in the $\vec{e}_a, \vec{e}_b, \vec{e}_{c^*}$ frame, the unity vectors along the positive ⟨*c*⟩ and ⟨*a**⟩ axes have the Cartesian coordinates

$$\begin{aligned}\vec{e}_c &= (-\sin\delta, 0, \cos\delta)\\ \vec{e}_{a^*} &= (\cos\delta, 0, \sin\delta)\end{aligned} \tag{12}$$

The magnetic field orientations for positive rotations over an angle θ in the {*bc*} and {*a***b*} planes are then given by

$$\begin{aligned}\vec{l}_{bc} &= (-\sin\theta\sin\delta, \cos\theta, \sin\theta\cos\delta)\\ \vec{l}_{a^*b} &= (\cos\theta\cos\delta, \sin\theta, \cos\theta\sin\delta)\end{aligned} \tag{13}$$

For rotation in the three crystallographic planes {*ab*}, {*bc*}, {*ca*}, Eq. (6) leads to the first and third expression in Eq. (9), but the second line should be replaced by

$$\begin{aligned}&M_{22} = \alpha_1 + \beta_1\\ &M_{33}\cos^2\delta + M_{11}\sin^2\delta - 2M_{13}\sin\delta\cos\delta = \alpha_1 - \beta_1\\ &M_{23}\cos\delta - M_{12}\sin\delta = \gamma_1\end{aligned} \tag{14}$$

This result was also obtained by Schonland [1] using $\varepsilon = -\delta$. If we assume ambiguity in the sign of $\gamma_3 = M_{12} = -\widetilde{M}_{12}$, all other matrix elements of the two best-fit tensors to the data points are identical, except for

$$\widetilde{M}_{23} = M_{23} - 2M_{12}\tan\delta \tag{15}$$

For rotations around the crystallographic axes in the {*a***b*}, {*bc**} and {*c***a*} planes, the second and third line of Eq. (9) should be combined with

$$\begin{aligned}&M_{11}\cos^2\delta + M_{33}\sin^2\delta + 2M_{13}\sin\delta\cos\delta = \alpha_3 + \beta_3\\ &M_{22} = \alpha_3 - \beta_3\\ &M_{12}\cos\delta + M_{23}\sin\delta = \gamma_3\end{aligned} \tag{16}$$

If we again assume ambiguity in the sign of γ_3, all matrix elements for the two best-fit matrices $\vec{M}$ are identical, except for

$$\widetilde{M}_{12} = -M_{12} - 2M_{23}\tan\delta \tag{17}$$

Knowing the ambiguity in $\vec{M}$, calculating the Schonland conjugate forms for $\vec{g}$ or $\vec{A}$ goes along the line set in Section 3.1.

In Fig. 4 we compare the angular dependence in the {*a***b*}, {*bc**} and {*c***a*} planes of the ENDOR transitions calculated with $\vec{A}$ tensor 1 in Table 2 and its monoclinic symmetric equivalent (filled and open circles) with that for the Schonland conjugated tensors calculated with Eq. (17) (full lines) and with tensor 2 from Table 2 (dashed lines), which is the Schonland conjugated form for rotation in the three orthogonal planes. δ is taken 13°, making the angle between ⟨*c*⟩ and ⟨*a*⟩ 103°. As expected, the full lines perfectly match the dots but the dashed lines do not fit at all in the {*a***b*} plane. So, in addition to the M_S multiplet and the microwave frequency, one should also carefully consider the planes in which the experiments

Table 3
Schonland conjugate tensors of the HFC tensor 1 in Table 2, calculated for the high (left) and low (right) frequency ENDOR transitions at various microwave frequencies ($g = 2$), considering the ambiguity in the sign of the off-diagonal M_{12}, arising when resonance frequency data are analysed in the {*ab*}, {*bc**} and {*c***a*} rotation planes

ν_{MW} (GHz)	$g_N\mu_N B_0$ (MHz)	$\widetilde{A}$ (MHz)	⟨*a*⟩	⟨*b*⟩	⟨*c**⟩	$\widetilde{A}$ (MHz)	⟨*a*⟩	⟨*b*⟩	⟨*c**⟩	$\Delta\theta$ (°)
1	*1.52*	*30.48*	−0.9121	0.2046	0.3553	*30.86*	−0.9160	0.1191	0.3830	*5.16*
		33.57	0.0693	0.9310	−0.3583	*33.81*	−0.0097	0.9480	−0.3181	*5.17*
		61.18	−0.4041	−0.3022	−0.8633	*61.03*	−0.4010	−0.2951	−0.8673	*0.50*
3	*4.56*	*30.19*	−0.9057	0.2591	0.3354	*31.33*	−0.9078	−0.0192	0.4190	*16.71*
		33.42	0.1197	0.9155	−0.3840	*34.25*	−0.1363	0.9582	−0.2515	*16.76*
		61.31	−0.4066	−0.3077	−0.8603	*60.84*	−0.3967	−0.2854	−0.8725	*1.56*
9.8	*14.9*	*29.58*	−0.8887	0.3478	0.2988	*27.44*	−0.6621	−0.6397	0.3905	*61.15*
		33.16	0.2014	0.8815	−0.4271	*43.48*	−0.6587	0.7452	0.1039	*61.32*
		61.62	−0.4119	−0.3194	−0.8534	*59.86*	−0.3574	−0.1884	−0.9147	*8.86*
34	*51.7*	*28.87*	−0.8681	0.4204	0.2641	*27.18*	0.8253	−0.5281	−0.2001	*7.59*
		32.92	0.2667	0.8435	−0.4662	*32.34*	0.3514	0.7576	−0.5501	*8.43*
		62.11	−0.4187	−0.3342	−0.8444	*65.56*	0.4421	0.3836	0.8108	*3.67*
94	*142.9*	*28.53*	−0.8584	0.4483	0.2493	*27.96*	−0.8435	0.4867	0.2272	*2.68*
		32.81	0.2908	0.8257	−0.4833	*32.62*	0.3223	0.7970	−0.5107	*2.90*
		62.44	−0.4225	−0.3424	−0.8392	*63.23*	−0.4297	−0.3576	−0.8292	*1.12*
270	*410.5*	*28.37*	−0.8541	0.4599	0.2429	*28.17*	−0.8489	0.4733	0.2352	*0.93*
		32.76	0.3006	0.8176	−0.4910	*32.70*	0.3116	0.8077	−0.5005	*1.01*
		62.63	−0.4244	−0.3464	−0.8366	*62.89*	−0.4268	−0.3516	−0.8332	*0.38*

The last column gives the deviation in principal directions between the two tensors in the row. The tensors at 9.8 GHz are identical to tensors 2 and 3 in Table 2.

have been carried out when calculating the Schonland conjugate $\overleftrightarrow{A}$ tensor. Furthermore, it may be easily verified that when $(\vec{e}_{a^*}, \vec{e}_b, \vec{e}_c)$ is chosen as reference frame for representation of the $\overleftrightarrow{g}$ and/or $\overleftrightarrow{A}$ tensors, expressions identical to (15) and (17) are found, except for a sign change in the second term on the right hand side.

3.3. Lifting the degeneracy by rotating in tilted planes

As a final point, it will be illustrated that the degeneracy between the two best-fit solutions is lifted, along with that of the resonance fields or frequencies for symmetry-related centres, when rotating in tilted planes. So far, the role of symmetry-related centres in deriving the equations has not been explicitly considered, but the simulations demonstrated that the Schonland conjugate of a symmetry-related tensor is the symmetry-related of the Schonland conjugate. This is obvious in Figs. 1, 2 and 4 and can, for the special case of rotation in three orthogonal planes, be verified in Table 1. For the case of monoclinic crystals considered in Section 3.2, one may verify that for the symmetry-related centre, which has $\overline{M}_{12} = -M_{12}, \overline{M}_{13} = M_{13}$ and $\overline{M}_{23} = -M_{23}$, Eqs. (14) and (16) still lead to (15) and (17). On the other hand, rotating outside the $\{c^*a\}$ plane for the same monoclinic crystal, e.g. from $(0, \sin\varepsilon, \cos\varepsilon)$ to $(1,0,0)$ leads to the expressions

$$\begin{aligned} &M_{33}\cos^2\varepsilon + M_{22}\sin^2\varepsilon + 2M_{23}\sin\varepsilon\cos\varepsilon = \alpha_2 + \beta_2 \\ &M_{11} = \alpha_2 - \beta_2 \\ &M_{13}\cos\varepsilon + M_{12}\sin\varepsilon = \gamma_2 \end{aligned} \tag{18}$$

to be combined with, e.g. the first and second line of Eq. 9. Again considering an ambiguity in the sign of γ_3, the two best-fit solutions for one site differ in the elements

$$\begin{aligned} &\widetilde{M}_{12} = -M_{12} \\ &\widetilde{M}_{13} = M_{13} + 2M_{12}\tan\varepsilon \end{aligned} \tag{19}$$

The symmetry-related tensor $\overleftrightarrow{\overline{M}}$ and its Schonland conjugate $\overleftrightarrow{\widetilde{\overline{M}}}$ have to be related by the same equations. However, this leads to the conclusion that the Schonland conjugate tensors for the two symmetry-related centres are not related by symmetry, because

$$\begin{aligned} \widetilde{\overline{M}}_{13} &= \overline{M}_{13} + 2\overline{M}_{12}\tan\varepsilon = M_{13} - 2M_{12}\tan\varepsilon \\ &\neq \overline{\widetilde{M}}_{13} = \widetilde{M}_{13} = M_{13} + 2M_{12}\tan\varepsilon \end{aligned} \tag{20}$$

It should further be noted from the first line in Eq. (18), that the angular dependences of the two symmetry-related centres no longer coincide, as α and β should differ, since $\overline{M}_{23} = -M_{23}$. This lifting of the degeneracy is clearly observable in Fig. 5. Here, we compare simulated ENDOR angular dependences of the two symmetry-related sites for protons with a HFC tensor 1 in Table 2 and its Schonland conjugate according to Eq. (19). A small tilting angle of $\varepsilon = 2°$ already leads to a significant difference in the tilted $\{c^*a\}$ plane: the symbols and lines coincide for only one of the symmetry-related centres. One can verify that for monoclinic crystals the ambiguity generally is also lifted when one of the rotation planes is not orthogonal to $\{c^*a\}$. For orthorhombic crystals, a similar lifting of the degeneracy is found for angular dependences in planes slightly tilted away from $\{ab\}$, $\{bc\}$ or $\{ca\}$ in the case of four symmetry-related centres.

In spite of this apparent advantage of tilted planes, measurements in crystal symmetry planes and directions should still be preferred, because crystals can be very accurately aligned to such orientations, just due to actual degeneracy of transitions. Inaccuracies in orientation and adjustment of the rotation planes in the fitting will inevitably lead to higher fitting errors and possibly also to additional (local) minima in the total error. Moreover, for systems where a large number of very similar paramagnetic centres are present with partially overlapping EPR and ENDOR spectra, accurate orientation to the $\langle a\rangle$, $\langle b\rangle$ and $\langle c^{(*)}\rangle$ axes where angular dependences of the interactions in various planes meet, is absolutely necessary, and reducing the number of lines by coincidence for symmetry-related centres may considerably facilitate the analysis.

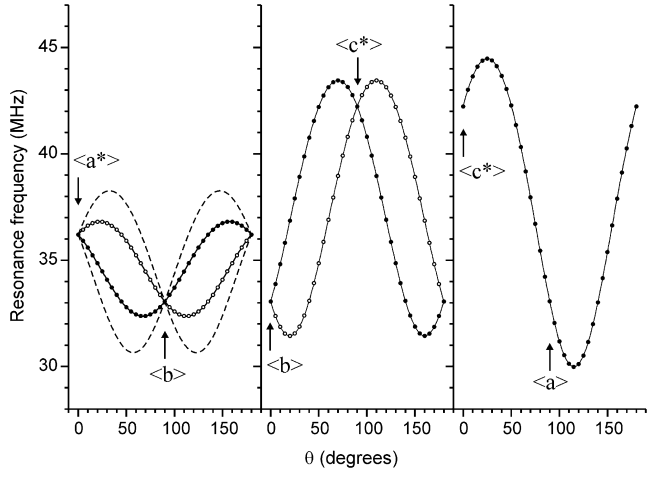

Fig. 4. Angular dependence in $\{a^*b\}$, $\{bc^*\}$ and $\{c^*a\}$ planes of the high frequency ENDOR branches for a non-symmetric centre with $S = 1/2$ interacting with a ^{1}H nucleus in a monoclinic crystal, calculated at a microwave frequency of 9.8 GHz (350 mT for $g = 2$). *Symbols:* For one of the symmetry-related sites, the interaction is parameterized by the tensor 1 in Table 2 (filled circles) and for the other by its monoclinic symmetry-related tensor (open circles). *Lines:* Simulations for the two symmetry-related centres, the interaction for one of which is parameterized by the Schonland conjugate tensor calculated using Eq. (17) (full lines). For comparison, the simulation with the Schonland conjugate tensor in case of rotation in three orthogonal planes (tensor 2 in Table 2) is also shown (dashed lines).

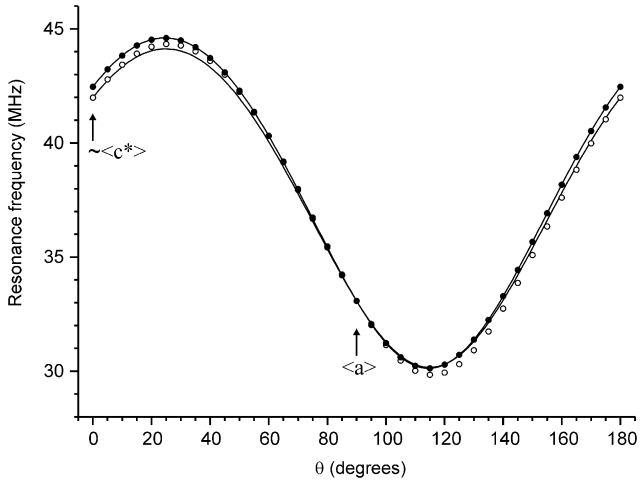

Fig. 5. Angular dependence in a slightly misaligned $\{c^*a\}$ plane (poles $\theta = 92°$ and $\phi = 90°$) of ENDOR frequencies calculated for a non-symmetric centre with $S = 1/2$ interacting with a ^{1}H nucleus. *Symbols:* With tensor 1 in Table 2 as $\overleftrightarrow{A}$ for one of the symmetry-related centres (filled circles) and its monoclinic symmetry-related $(\overleftrightarrow{\overline{A}})$ for the other (open circles). *Lines:* With the Schonland conjugate of tensor 1 in Table 2 for one of the symmetry-related centres $(\overleftrightarrow{\widetilde{A}})$ and its monoclinic symmetry-related for the other $(\overleftrightarrow{\overline{\widetilde{A}}})$. The discrepancy between the angular dependences for the second site (open circles and full lines) demonstrates that for this tilted plane, the symmetry-related of the Schonland conjugate tensor is not the Schonland conjugate of the symmetry-related tensor.

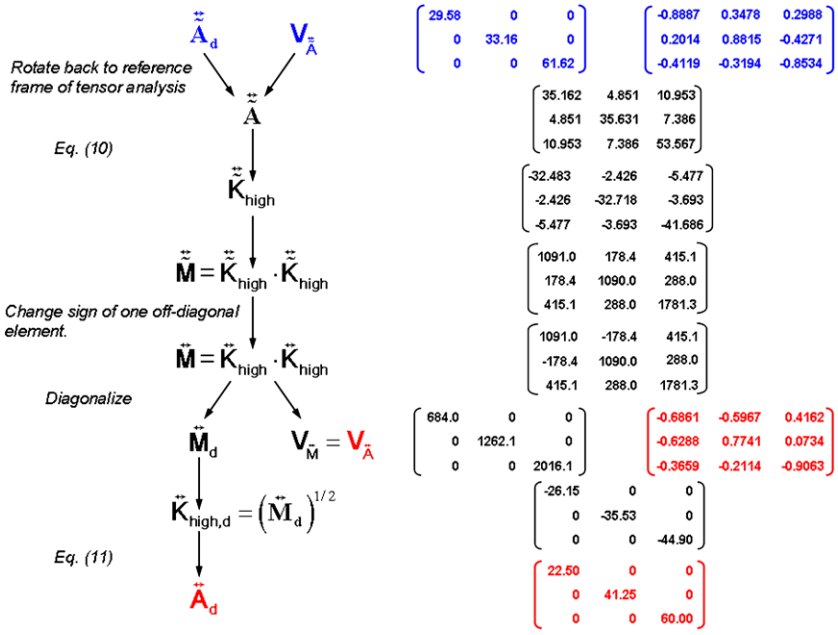

Fig. A. Starting from tensor 2 in Table 1, the Schonland conjugate tensor (tensor 1 in Table 2) is calculated under the assumption that high frequency ENDOR branches (K_{high}, Eqs. (10), (11)) are used in the analysis, and for experimental data in $\{ab\}$, $\{bc^*\}$ and $\{c^*a\}$ planes. $g_N\mu_N B_0$ = 14.902 MHz (B_0 = 350 mT, g = 2 at 9.8 GHz). For the low frequency ENDOR branches (K_{low}), the first term on the right hand side of Eq. (10) and the complete right hand side of Eq. (11) should be changed in sign, as explained in the text. For experimental data in the $\{ab\}$, $\{bc\}$ and $\{ca\}$ planes, Schonland conjugation of $\overleftrightarrow{M}$ should be performed using Eq. (15), and for the $\{a^*b\}$, $\{bc^*\}$ and $\{c^*a\}$ planes using Eq. (17).

4. Conclusions

In this paper, the possibility of obtaining two distinct, not symmetry-related, best-fit $\overleftrightarrow{A}$ tensor solutions from angular dependent ENDOR measurements is explored for $I = 1/2$ nuclei interacting with an electronic spin $S = 1/2$ with (quasi) isotropic $\overleftrightarrow{g}$ tensor. This problem is particularly important in theoretical interpretations and/or when radical identification based on "first principles" reproduction of $\overleftrightarrow{A}$ tensors is envisaged. This is illustrated in an example where alternative Schonland conjugate forms of an $\overleftrightarrow{A}$ tensor would lead to identification of the interacting nucleus as either a β-hydroxyl or an α-proton. We have confined the discussion to non-symmetric paramagnetic centres in orthorhombic and monoclinic crystals, for which Schonland reported a possible ambiguity for the $\overleftrightarrow{g}$ tensor when restricting the measurements to three symmetry planes (see Section 3). If in the ENDOR measurements the nuclear transitions within the two M_S multiplets both may be observed, for each of them two best-fit $\overleftrightarrow{A}$ tensors can be found, but in general only one tensor fits both the high and low frequency branches. Thus, in principle the Schonland ambiguity for $\overleftrightarrow{A}$ tensors from ENDOR experiments does not exist. However, in practice tensors very often are obtained by fitting transitions within only one of the M_S multiplets, the other not being measured or difficult to analyse because of overlap with other lines, and an ambiguity in the fitting result may exist. We have shown how to calculate the other best-fit tensor, which we call Schonland conjugate, for a given best-fit $\overleftrightarrow{A}$ tensor determined from ENDOR experiments. The result depends on various details of the experiment:

(1) whether the high or low frequency branches were fitted;
(2) the magnetic field/microwave frequency;
(3) the rotation planes in which the data were gathered and also the choice of reference frame.

The results in this paper should encourage ENDOR spectroscopists to measure and analyse ENDOR data in both M_S multiplets, or, when this is not possible or conclusive (see limiting cases), to complement their measurements by experiments in a fourth plane or at another microwave frequency (less discriminating). The paper should enable computational researchers to recognize experimental circumstances which lead to the Schonland ambiguity and provide the means for calculating the other best-fitting tensors where these have not been considered in literature, without aid of simulation and or fitting tools.

Acknowledgment

The authors thank the Flemish Research Foundation (FWO-Vlaanderen) for financial support.

Appendix A

Fig. A.

References

[1] D.S. Schonland, On the determination of principal g-values in electron spin resonance, Proc. Phys. Soc. Lond. 73 (1959) 788–792.
[2] J.R. Morton, K.F. Preston, EPR spectroscopy of single crystals using a two-circle goniometer, J. Magn. Reson. 52 (1983) 457–474.
[3] W.G. Waller, M.T. Rogers, Generalization of methods for determining g tensors, J. Magn. Reson. 9 (1972) 92–107.
[4] N.M. Atherton, Principles of Electron Spin Resonance, Ellis Horwood–Prentice Hall, 1993.
[5] A. Lund, T. Vänngård, Note on the determination of principal fine and hyperfine coupling constants in ESR, J. Chem. Phys. 42 (1965) 2979–2980.
[6] H. De Cooman, E. Pauwels, H. Vrielinck, E. Sagstuen, F. Callens, M. Waroquier, Identification and conformational study of stable radiation-induced defects in sucrose single crystals using density functional theory calculations of electron magnetic resonance parameters, J. Phys. Chem. B 112 (2008) 7298–7307.
[7] H. De Cooman, E. Pauwels, H. Vrielinck, A. Dimitrova, N. Yordanov, E. Sagstuen, M. Waroquier, F. Callens, Radiation-induced defects in sucrose single crystals, revisited: a combined electron magnetic resonance and density functional theory study, Spectrochim. Acta A 69 (2008) 1372–1383.
[8] M. Tarpan, E. Sagstuen, E. Pauwels, H. Vrielinck, M. Waroquier, F. Callens, Combined electron magnetic resonance and density functional theory study of

10 K X-irradiated β-D-fructose single crystals, J. Phys. Chem. A 112 (2008) 3898–3905.
[9] E. Pauwels, R. Declerck, V. Van Speybroeck, M. Waroquier, Evidence for a Grotthuss-like mechanism in the formation of the rhamnose alkoxy radical based on periodic DFT calculations, Radiat. Res. 169 (2008) 8–18.
[10] K.T. Øhman, A. Sanderud, E.O. Hole, E. Sagstuen, Single crystals of L-O-serine phosphate X-irradiated at low temperatures: EPR, ENDOR, EIE and DFT studies, J. Phys. Chem. A 110 (2006) 9585–9596.
[11] N. Jayatilaka, W.H. Nelson, Structure of radicals from X-irradiated guanine derivatives: an experimental and computational study of sodium guanosine dihydrate single crystals, J. Phys Chem. B 111 (2007) 800–810.
[12] H. De Cooman, G. Vanhaelewyn, E. Pauwels, E. Sagstuen, M. Waroquier, F. Callens, Radiation-induced radicals in glucose-1-phosphate (I). Electron paramagnetic resonance and electron nuclear double resonance analysis of in situ X-irradiated single crystals at 77 K, J. Phys. Chem. B, accepted for publication.
[13] E. Pauwels, H. De Cooman, G. Vanhaelewyn, E. Sagstuen, F. Callens, M. Waroquier, Radiation-induced radicals in glucose-1-phosphate (II). DFT analysis of structures and possible formation mechanisms, J. Phys. Chem. B, accepted for publication.
[14] W. Gordy, Theory and Applications of Electron Spin Resonance Techniques of Chemistry (volume XV), John Wiley and Sons, Inc., 1980.
[15] S. Stoll, A. Schweiger, EasySpin, a comprehensive software package for spectral simulation and analysis in EPR, J. Magn. Reson. 178 (2006) 42–55.
[16] J.A. Weil, J.H. Anderson, Direct field effects in electron paramagnetic resonance spectra, J. Chem. Phys. 35 (1961) 1410–1417.
[17] M. Iwasaki, Second-order perturbation treatment of the general spin hamiltonian in an arbitrary coordinate system, J. Magn. Reson. 16 (1974) 417–423.
[18] J.A. Weil, Comments on second-order spin-Hamiltonian energies, J. Magn. Reson. 18 (1975) 113–116.
[19] B. Epel, P. Manikandan, P.M.H. Kroneck, D. Goldfarb, High-field ENDOR and the sign of the hyperfine coupling, Appl. Magn. Reson. 21 (2001) 287–297.
[20] T.C. Yang, B.M. Hoffman, A Davies/Hahn multi-sequence for studies of spin relaxation in pulsed ENDOR, J. Magn. Reson. 181 (2006) 280–286.
[21] J.J.L. Morton, N.S. Lees, B.M. Hoffman, S. Stoll, Nuclear relaxation effects in davies ENDOR variants, J. Magn. Reson. 191 (2008) 315–321.
[22] S.E. Locher, H.C. Box, ESR-ENDOR studies of X-irradiated glucose-1-phosphate dipotassium salt, J. Chem. Phys. 72 (1980) 828–832.